TIME-DEPENDENT FLOW AROUND A CIRCULAR CYLINDER ACCELERATED UNIFORMLY FROM ONE STEADY SPEED TO ANOTHER

HONJI, Hiroyuki
Research Institute for Applied Mechanics, Kyushu University : Lecturer

TANEDA, Sadatoshi
Research Institute for Applied Mechanics, Kyushu University : Professor

https://doi.org/10.5109/7170236

出版情報：Reports of Research Institute for Applied Mechanics. 17 (59), pp.187-193, 1969. 九州大学応用力学研究所
バージョン：

Reports of Research Institute for Applied Mechanics
Vol. XVII, No. 59, 1969

TIME-DEPENDENT FLOW AROUND A CIRCULAR CYLINDER ACCELERATED UNIFORMLY FROM ONE STEADY SPEED TO ANOTHER+

By Hiroyuki HONJI* and Sadatoshi TANEDA**

Unsteady flow around a circular cylinder accelerated from one steady speed to another was investigated experimentally using flow visualization techniques. The experiment was carried out in a water tank. The initially prescribed Reynolds number was varied between 19 and 89, and the dimensionless acceleration between 1.0×10^2 and 3.0×10^4. The following facts were found. Immediately after the cylinder is given an acceleration, an inviscid flow pattern appears near the cylinder and the initial vortices are left downstream. Then the new twin vortex formation begins immediately behind the cylinder, and the secondly formed vortices develop downstream in a manner similar to the case of start from rest. The change of the flow pattern is characterized by the initially prescribed Reynolds number and the applied acceleration.

1. Introduction

Recently many papers have been concerned with the unsteady boundary layer growth on a cylindrical obstacle which is started from rest either impulsively or with uniform acceleration.[1)~6)] The starting flow of a circular cylinder having zero initially prescribed velocity thus has been clarified to a considerable extent both theoretically and experimentally. Naturally, the problem may be generalized to a case in which the cylinder is accelerated from one steady speed to another larger speed. In this work such a problem was studied experimentally, and some results obtained are presented including many photographs of unsteady flow patterns.

2. Experimental Method

The experiment was carried out using a flow visualization method in a 50 cm $\times$ 50 cm $\times$ 5 m water tank. Photo. 1 shows the side view of the apparatus.

+ This work was read at the Annual Meeting of the Physical Society of Japan held in Nagoya (October 10, 1969).

* Lecturer, **Professor, Research Institute for Applied Mechanics, Kyushu University, Fukuoka, Japan.

A model circular cylinder made from an ebonite rod of 30 cm in length and 1.0 or 1.5 cm in diameter was attached vertically to a carriage, and moved in the water tank. For flow visualization the aluminum dust method was used. Many photographs of the consecutive flow patterns were taken using a motor-drive camera which was fixed to the carriage. The time interval between the onset of acceleration and the middle of the time of exposure (hereafter referred to as "the time of observation") was measured by reading oscillograms of electric signals from an electrical switch unit of the camera and from a speed control unit indicating the onset of acceleration.

3. Results and Discussions

Unsteady flows were examined with respect to the following two types of series of experiment (Fig. 1 should be referred).

(1) The cylinder is accelerated from one steady speed to another with different accelerations (Fig. 1.1).

(2) The cylinder is accelerated from one steady speed to other different speeds with a constant acceleration (Fig. 1.2).

These are referred to as Case (1) and Case (2) respectively in this paper. The cylinder speed, the acceleration and the time should be replaced by the Reynolds number R, the dimensionless acceleration α, and the dimensionless time τ respectively; these determine the unsteady flow field directly. Before presenting the results obtained, the parameters are here defined as $R_i = U_i d/\nu$,

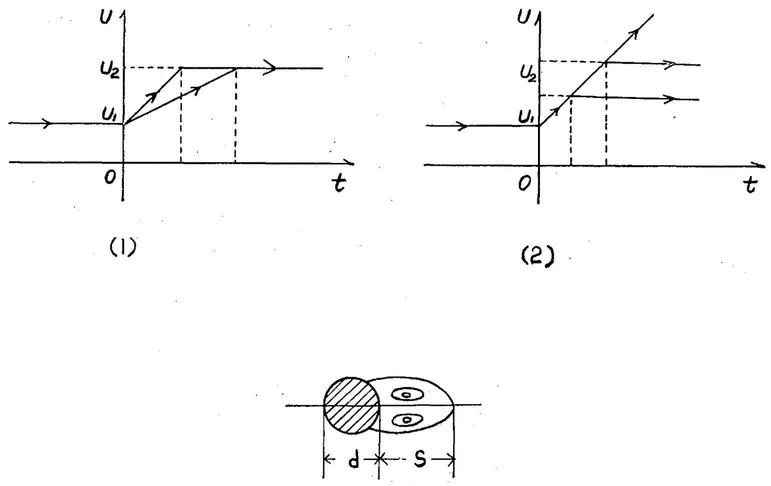

Fig. 1. Two types of series of experiment, and definition of the vortex length S.

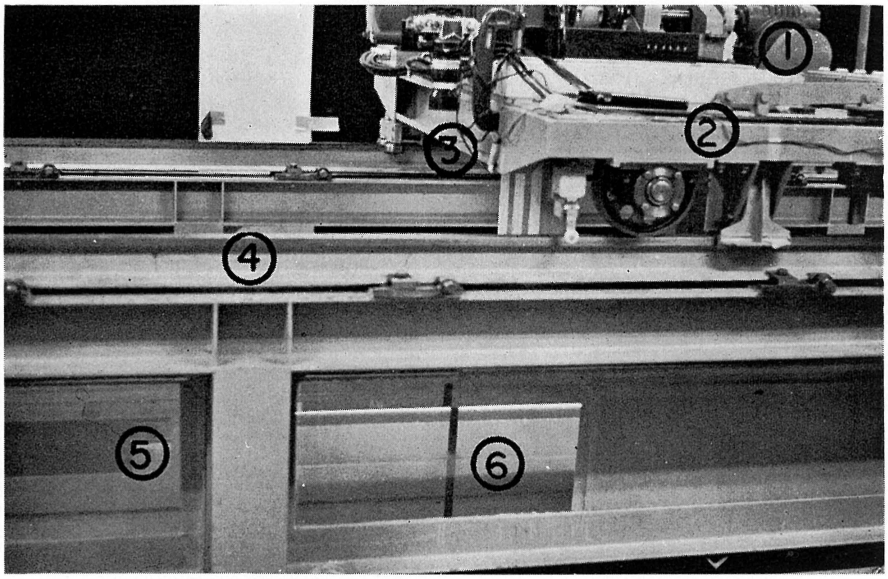

Photo. 1. Side view of the experimental apparatus.

(1) Driving motor (2) Carriage
(3) Camera (4) Rail
(5) Water tank (6) Test circular cylinder

(*Facing p.* 188)

$\alpha=d^3a/\nu^2$, and $\tau=\nu t/d^2$, where U_i is the cylinder speed (i designates 1 or 2 according to the initially prescribed velocity or the secondly prescribed one respectively), d the cylinder diameter, ν the kinematic viscosity, a the cylinder acceleration, and t the time of observation. The dimensionless vortex length S/d is correlated with the dimensionless parameters above defined as,

$$S/d=f(R_1,\ R_2,\ \alpha,\ \tau), \tag{1}$$

where f denotes some function. Eq. (1) will be used later in arranging the experimental data concerned with the vortex length.

Some examples of unsteady flow patterns are presented with respect to Cases (1) and (2). Photo. 2 (a–d) shows the variation of the flow pattern when R_1 gives the twin vortices, and R_2 the Kármán vortex street. Photo. 2 (a) shows the ordinary steady twin vortices formed behind the test cylinder moving with a constant speed. Immediately the cylinder is accelerated, the flow pattern changes suddenly as will be seen from Photo. 2 (b); the vortex pattern disappears apparently and the pattern similar to that of the inviscid flow appears near the cylinder, in spite of the existence of the distributed vorticity due to the steady motion before the acceleration. As time advances, however, the new vortex formation begins, and the entirely new vortices develop downstream. This situation will be seen from the remaining pictures of Photo. 2. When R_2 exceeds 40, a secondly developed twin vortex pattern turns into a periodic vortex pattern.

The change of the flow pattern due to a small acceleration is presented in Photos. 3 (a) and (b), in which the former shows the established steady twin vortices, and the latter the flow pattern immediately after the onset of acceleration. As will be seen from these pictures, the inviscid flow pattern in this case does not appear clearly. This means that the apparent appearance of the inviscid flow pattern depends on α. The quantitative determination of the critical acceleration for the appearance of the inviscid flow pattern was not made in the present investigation; the exact determination using such photographs as illustrated in Photo. 3 (b) seems to be very difficult.

When both R_1 and R_2 give the Kármán vortex street, the flow pattern variation shows somewhat a different feature, as shown in Photo. 4 (a–d). Photo. 4 (a) shows the periodic vortex wake behind the cylinder moving steadily, Photo. 4 (b) the flow pattern immediately after the onset of acceleration. Apparently the wake turbulence is reduced and the new twin vortices are being developed. Photos. 4 (c) and (d) indicate that the secondly established vortices grow into the periodic ones again.

As has been illustrated hitherto in many photographs, initially established vortices are seemingly lost to sight and a flow pattern similar to that of an inviscid flow appears around a circular cylinder, when it is accelerated uniformly from a steady speed. On the other hand, the Helmholtz theorem of permanence of vorticity indicates that the fluid particles which constitutes the already established vortices continues to have vorticity for a fairly long time.[7] Thus, the next task may be to trace the initially established vortices more closely. In order to visualize the process taking place in the flow after acceleration more clearly, another flow visualization was carried out using both the aluminum dust and condensed milk which visualizes streaklines simultaneously.

Photo. 5 (a–h) and Photo. 6 (a–f) show the flow patterns visualized by using the above described method. Photo. 5 shows the variation in time of the flow pattern, when the cylinder is accelerated from a steady speed corresponding to that within the twin vortex range. Photo. 5 (b) shows the unsteady flow pattern immediately after the acceleration; the initially established vortex is blown downstream, and at the same time the inviscid flow is being realized as will be seen from the paths of aluminum dusts. Photo. 6 shows the similar phenomena at the pure Kármán range. Even for the Reynolds numbers larger than about 40 at which the wake begins to oscillate, the onset of acceleration makes it possible to form the twin vortices.

Further work was carried out to trace the initial vortices; the flow was viewed relative to the undisturbed water. Instead of attaching the camera to the carriage, it was located independently of the moving system. For comparison, the flow field around a circular cylinder started from rest is presented in Photo. 7, which shows a typical symmetrical vortex-pair. Photo. 8 (a–c) shows the vortex patterns of successive runs with different delay times. The flow pattern of the circular cylinder moving steadily is shown in Photo. 8 (a), in which the vortex centers are displaced slightly downstream due to the viscosity. Photo. 8 (b) shows the flow pattern immediately after the onset of acceleration. This picture shows that a vortex-pair similar to that illustrated in Photo. 7 is formed around the cylinder. The strength of the new vortices is so large that the traces of the initial vortices cannot be observed clearly. However, Photo. 8 (c), continued from Photo. 8 (b), gives an evidence, though inconspicuous, of the "missing" vortices in the wake far from the cylinder.

With a slightly larger value of R_1, the traces of the initial vortices become more distinct as will be seen from Photo. 9. When both R_1 and R_2 give the pure Kármán vortex street, the initial vortices left in the far wake are observed clearly, as will be seen from Photo. 10. Photo. 10 (a) shows the periodic vortex wake behind the steady circular cylinder viewed relative to the undisturbed water. Photo. 10 (b) shows again the new vortex-pair formation after the acceleration, and Photo. 10 (c) the detached vortices in the far wake.

Many observational evidences thus described indicate the following facts. After acceleration a new inviscid flow field is superposed on an already established viscous one. Then the initial vortices are left downstream, while the new vortex formation begins on the cylinder surface. As time elapses further, these vortices develop downstream until the final flow regime is completed.

The phenomenon of appearance of the inviscid flow pattern may be interpreted as follows. Immediately after acceleration of a cylinder, the dominant terms in the Navier-Stokes equations governing the neighbouring flow field caused by the acceleration are

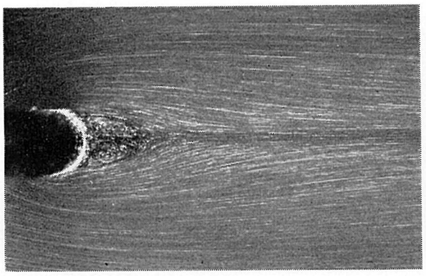

(a) Standing vortex behind the cylinder moving steadily at $R_1=20.0$.

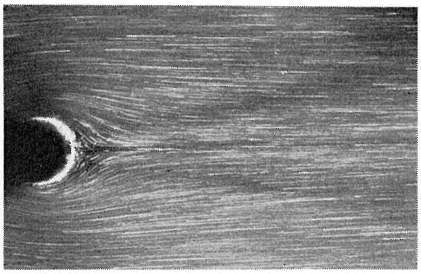

(b) Flow around the cylinder immediately after the onset of acceleration; $t=3.80$ s and $\tau=3.31\times10^{-2}$.

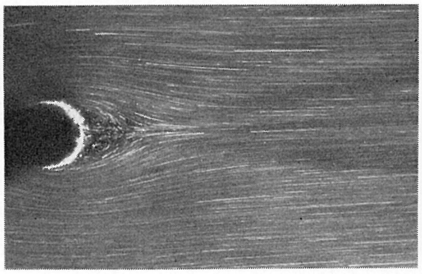

(c) Growth of the new twin vortices; $t=6.47$ s and $\tau=5.63\times10^{-2}$.

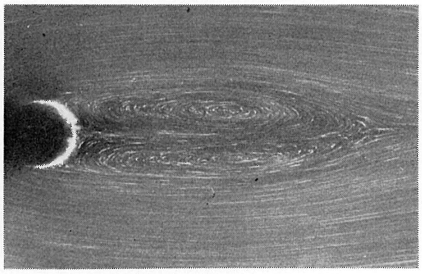

(d) Developed unsteady vortices; $t=24.7$ s and $\tau=2.15\times10^{-1}$.

Photo. 2. Consecutive stages of the flow around a circular cylinder accelerated from one steady speed to another; $U_1=0.174$ cm/s, $U_2=0.968$ cm/s, $a=0.0853$ cm/s^2, $d=1.00$ cm and t_e (=time of exposure) = 2 s, $R_1=20.0$, $R_2=111$ and $\alpha=1.13\times10^3$.

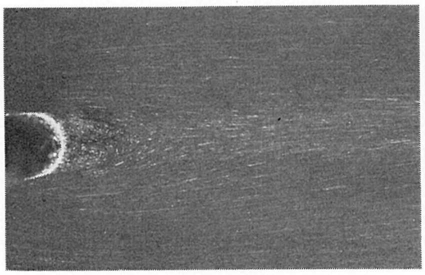

(a) Steady vortex at $R_1=20.3$.

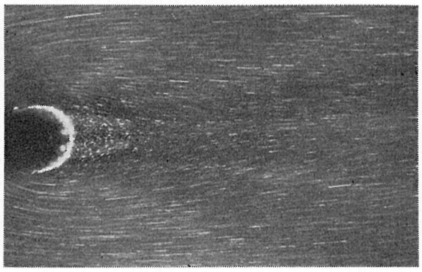

(b) Flow immediately after the onset of acceleration; $t=8.30$ s and $\tau=7.14\times10^{-2}$.

Photo. 3. Change of the flow pattern due to a small magnitude of acceleration; $U_1=0.175$ cm/s, $U_2=0.276$cm/s, $a=0.010$ cm/s^2, d=1.00 cm, $t_e=2$ s, $R_1=20.3$, $R_2=32.1$ and $\alpha=1.35\times10^2$.

(*Facing p.* 190)

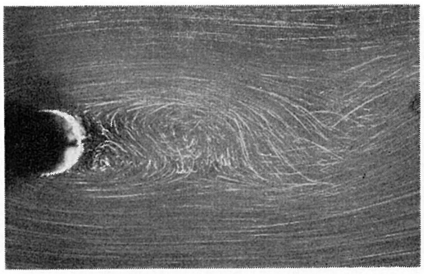

(a) Periodic vortices behind the cylinder moving steadily at R_1 $=89.2$.

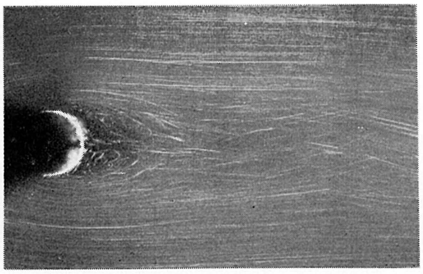

(b) Flow immediately after the onset of acceleration; $t=1.32$ s and $\tau=$ 1.12×10^{-2}.

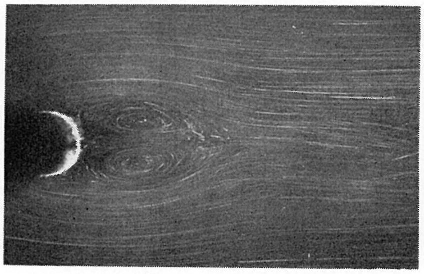

(c) Growth of the secondly established twin vortices; $t=3.80$ s and $\tau=3.23\times10^{-2}$.

(d) Final stage of the flow at $R_2=111$; $t=11.5$ s and $\tau=9.78\times10^{-2}$.

Photo. 4. Consecutive stages of the flow around a circular cylinder, whose velocity is changed within the pure Kármán range; $U_1=0.759$ cm/s, $U_2=1.47$ cm/s, $a=1.98$ cm/s^2, $d=1.00$ cm, $t_e=2$ s, $R_1=89.2$, $R_2=173$ and $\alpha=2.74\times10^4$.

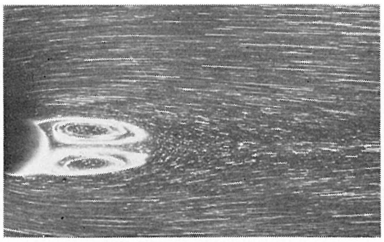

(a) Steady vortex at $R_1=33.6$.

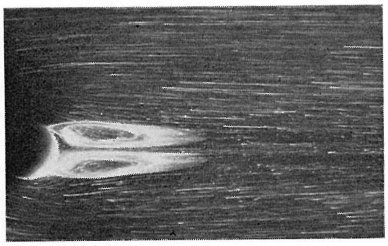

(b) $t=0.96$ s and $\tau=9.70\times10^{-3}$.

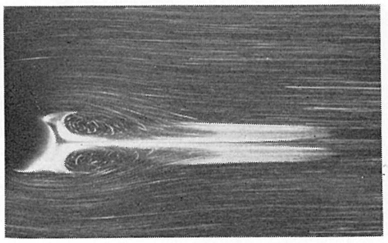

(c) $t=4.51$ s and $\tau=4.56\times10^{-2}$.

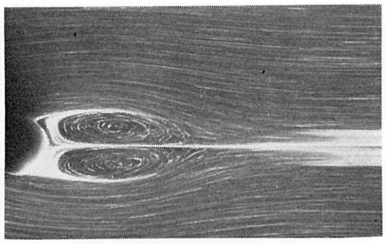

(d) $t=7.94$ s and $\tau=8.02\times10^{-2}$.

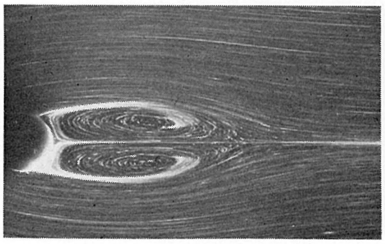

(e) $t=11.4$ s and $\tau=1.15\times10^{-1}$.

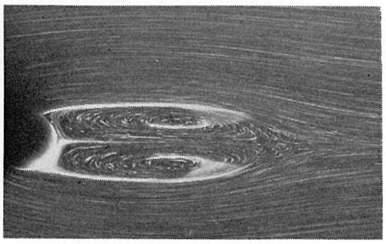

(f) $t=15.0$ s and $\tau=1.52\times10^{-1}$.

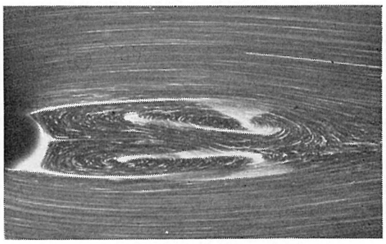

(g) $t=22.0$ s and $\tau=2.22\times10^{-1}$.

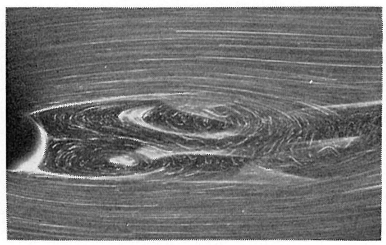

(h) $t=29.0$ s and $\tau=2.93\times10^{-1}$.

Photo. 5. Consecutive stages of the flow around a circular cylinder accelerated from one steady speed to another. Streak lines visualized with condensed milk are superposed on the aluminum-dust flow patterns; $U_1=0.339$ cm/s, $U_2=0.994$ cm/s, $a=0.298$ cm/s^2, $d=1.00$ cm, $t_e=3$s, $R_1=33.6$, $R_2=98.4$ and $\alpha=2.92\times10^3$.

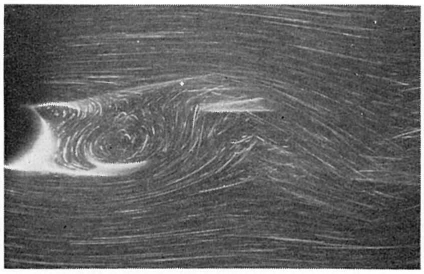

(a) Periodic vortices at $R_1=73.5$.

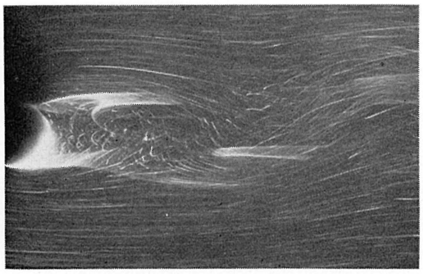

(b) $t=0.56$ s and $\tau=5.66\times10^{-3}$.

(c) $t=3.24$ s and $\tau=3.27\times10^{-2}$.

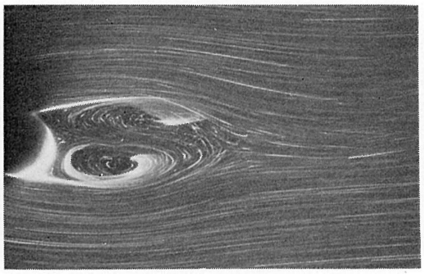

(d) $t=6.04$ s and $\tau=6.10\times10^{-2}$.

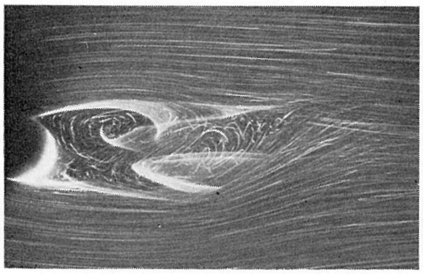

(e) $t=8.55$ s and $\tau=8.64\times10^{-2}$.

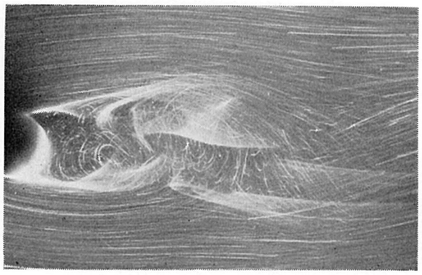

(f) $t=11.1$ s and $\tau=1.12\times10^{-1}$.

Photo. 6. Like Photo. 5, but both R_1 and R_2 are those within the pure Kármán range; $U_1=0.735$ cm/s, $U_2=1.50$ cm/s, a$=0.348$ cm/s^2, $d=1.00$ cm, $t_e=2$ s, $R_1=72.8$, $R_2=149$ and $\alpha=3.41\times10^3$.

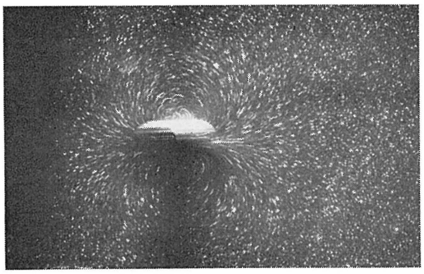

Photo. 7. Flow pattern of a circular cylinder started from rest. The camera is at rest with respect to the undisturbed water; $U_2=0.688$ cm/s, $a=0.459$ cm/s^2, $d=1.50$ cm, $t=3.92$ s, $t_e=2$ s, $R_2=115$, $\tau=1.57\times10^{-2}$ and $\alpha=1.91\times10^4$.

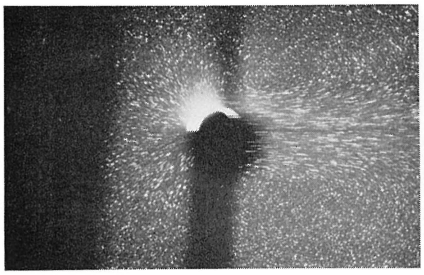

(a) Steady flow pattern at $R_1=30.0$.

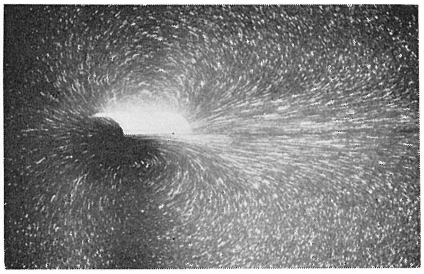

(b) $t=4.32$ s and $\tau=1.69\times10^{-2}$.

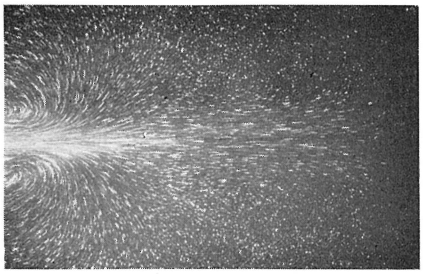

(c) $t=13.4$ s and $\tau=5.24\times10^{-2}$.

Photo. 8. Consecutive stages of the flow around a circular cylinder accelerated from one steady speed to another. The camera is at rest with respect to the undisturbed water; $U_1=0.176$ cm/s, $U_2=0.765$ cm/s, $a=0.160$ cm/s^2, $d=1.50$ cm, $t_e=2$ s, $R_1=30.0$, $R_2=130$ and $\alpha=6.97\times10^3$.

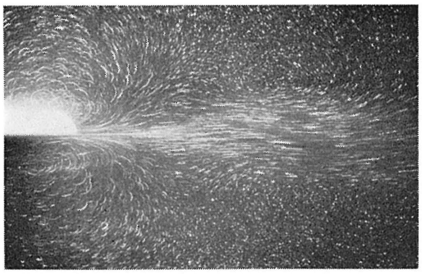

Photo. 9. Like Photo. 8, but R_1 is about twice that for Photo. 8; $U_1=0.347$ cm/s, $U_2=1.35$ cm/s, $a=0.531$ cm/s², $t=5.72$ s, $d=1.50$ cm, $t_e=2$ s, $R_1=59.1$, $R_2=229$, $\tau=2.24\times10^{-2}$ and $\alpha=2.31\times10^4$.

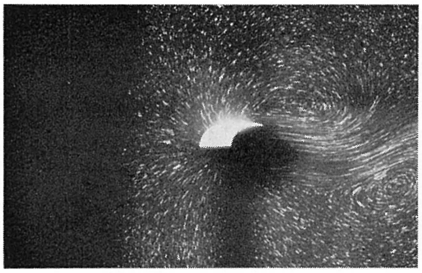

(a) Periodic vortices at $R_1=75.2$.

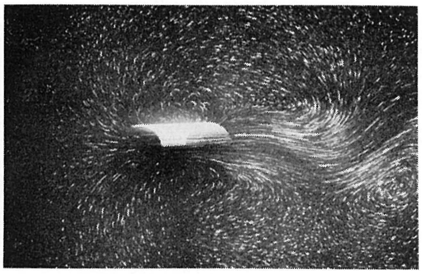

(b) $t=1.68$ s and $\tau=6.57\times10^{-3}$.

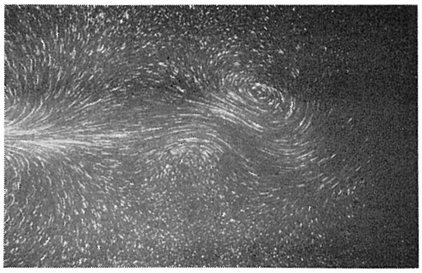

(c) $t=9.18$ s and $\tau=3.59\times10^{-2}$.

Photo. 10. Like Photo. 8, but both R_1 and R_2 are those within the pure Kármán range; $U_1=0.441$ cm/s, $U_2=1.27$ cm/s, $a=0.627$ cm/s², $d=1.50$ cm, $t_e=3$ s, $R_1=75.2$, $R_2=217$ and $\alpha=2.73\times10^4$.

$$\frac{\partial V}{\partial t} = -\frac{1}{\rho}\text{grad } p, \tag{2}$$

where V is the flow velocity, ρ the fluid density, and p the pressure. Eq. (2) indicates the realization of the inviscid flow pattern at least near the test body. As the cylinder moves upstream with the given acceleration, the vortices existing just before the initiation of acceleration are left in the wake.

Quantitative data obtained for Cases (1) and (2) are arranged based on Eq. (1). Fig. 2 shows the variation in time of the vortex length for the case $R_1 \simeq 20$ and $R_2 \simeq 32$, as an example of Case (1). At $\tau=0$ (the dimensionless time of the initiation of acceleration), the length of the already established twin vortices is reduced to zero apparently. Then the new vortex formation begins as already illustrated using many photographs. As τ increases, S/d of the new vortices increases until S/d corresponding to the final flow regime is reached. As will be seen from this figure, the phenomenon of slight overshoots is observed in the S/d-τ relationship just before S/d settle down in their final values. With the larger value of α, the shorter is the value of τ for establishing the final flow regime. Fig. 3 shows S/d plotted against τ for the case of $R_1 \simeq 20$ and $R_2 \simeq 110$, where the final stage of the flow is the Kármán vortex street.

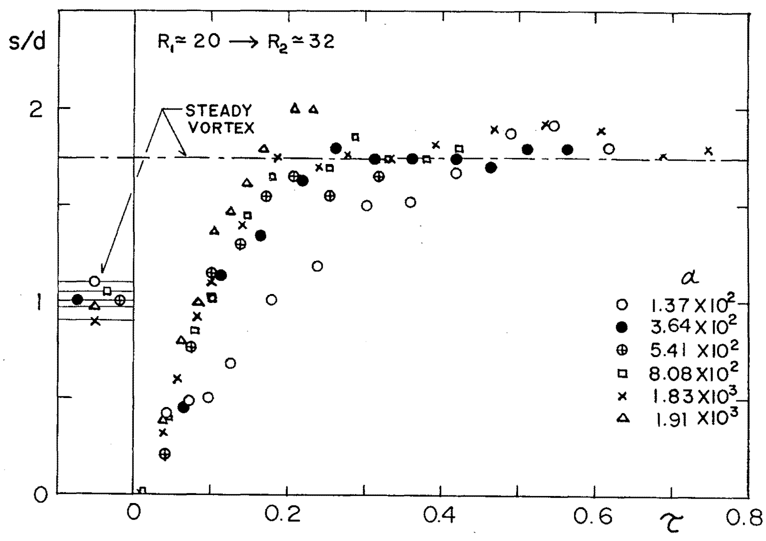

Fig. 2. The relationship between S/d and τ for an example of Case 1; both R_1 and R_2 are smaller than $R=40$, at which the twin vortices are changed into the periodic ones. The value of S/d at $\tau<0$ indicates the corresponding steady vortex.

Fig. 4 shows S/d plotted against τ for Case (2). For comparison, the S/d-τ curve for start-from-rest case at nearly the same α is illustrated. As is expected, this curve shows a slight delay in time of vortex growth, although its manner of τ dependence is not different from that for the case of acceleration from a steady speed.

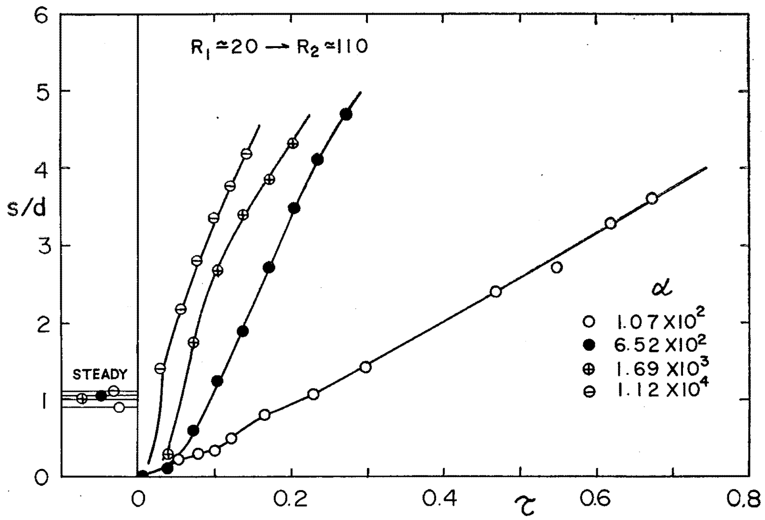

Fig. 3. The relationship between S/d and τ for an example of Case 1.

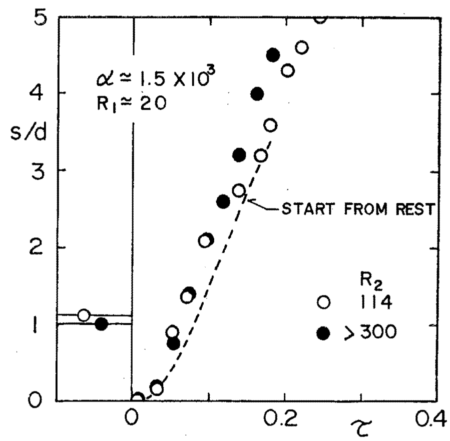

Fig. 4. The relationship between S/d and τ for an example of Case 2. The dotted line was drawn based on Ref. 6.

4. Conclusion

The time-dependent flows caused by unsteady motions of a circular cylinder accelerated from steady speed have been examined using many photographs of flow patterns. When the cylinder moving steadily is given an acceleration suddenly, the phenomenon of apparent disappearance of an already established vortex pattern occurs. Detailed observations, however, revealed that immediately after the onset of acceleration an inviscid flow pattern is superposed on the already established viscous flow pattern, and then the former turns into a new twin vortex pattern and the initial vortices are left downstream in the wake. The secondly appeared vortices grow downstream with time ; the mananer of their growth in length with time is essentially the same as that for the case of start from rest.

Acknowledgements

The authors wish to thank Mr. Koji Ishi-i for his collaboration through this work. The help of Miss. Hitomi Yanase is also acknowledged. This work was supported by the Grant-in-Aid for the Scientific Research from Ministry of Education.

References

1) L. Prandtle and O. Tietjens: *Applied Hydro-& Aeromechanics,* Dover (1957) 279.
2) R. B. Payne: J. Fluid Mech. 4 (1958) 81.
3) C. Y. Wang: J. Math. Phys. XLVI, 2 (1967) 195.
4) S. Taneda and H. Honji: Bull. Res. Inst. Appl. Mech. 30 (1968) 21, (in Japanese).
5) J. S. Son and T. J. Hanratty: J. Fluid Mech. 35 (1969) 369.
6) H. Honji and S. Taneda: J. Phys. Soc. Japan 27 (1969) 1668.
7) L. M. Milne-Thomson: *Theoretical Hydrodynamics,* McMillan (1968) 86.

(Received December 9, 1969)